



The normalized limit of detection in NMR spectroscopy

Piotr Lepucki^{a,*}, Adam P. Dioguardi^a, Daniil Karnaushenko^b, Oliver G. Schmidt^{b,c,d}, Hans-Joachim Grafe^a

^a IFW Dresden, Institut für Festkörperforschung, Helmholtzstraße 20, 01069 Dresden, Germany

^b IFW Dresden, Institut für Integrative Nanowissenschaften, Helmholtzstraße 20, 01069 Dresden, Germany

^c TU Dresden, Nanophysik, Häckelstraße 3, 01069 Dresden, Germany

^d TU Chemnitz, Material Systems for Nanoelectronics, Straße der Nationen 62, 09111 Chemnitz, Germany

ARTICLE INFO

Article history:

Received 12 March 2021

Revised 19 September 2021

Accepted 20 September 2021

Available online 28 September 2021

Keywords:

Nuclear magnetic resonance

Spectroscopy

Limit of detection

Signal-to-noise ratio SNR

Microcoil

ABSTRACT

We derive the normalized limit of detection for frequency space ($nLOD_f$) as a parameter to measure the sensitivity of an NMR spectroscopy setup. $nLOD_f$ is independent of measurement settings such as bandwidth or number of measurement points, and allows to compare performances of different setups. We demonstrate the usefulness of the new $nLOD_f$ by comparing the sensitivity of NMR setups from various publications, which all use microcoils. Finally, we want to propose a standard measurement and report format for the sensitivity of new NMR setups.

© 2021 The Authors. Published by Elsevier Inc. This is an open access article under the CC BY-NC-ND license (<http://creativecommons.org/licenses/by-nc-nd/4.0/>).

1. Introduction

The signal-to-noise ratio (SNR) of an NMR measurement is not a good parameter to compare sensitivities of different NMR systems. It depends on many parameters, like sample type, number of performed scans or the bandwidth of the spectrometer. Furthermore, it makes a difference if the SNR is measured in time space or frequency space. In the former case the SNR is measured on all resonating spins, which especially for spectroscopy could give a false impression of the true sensitivity of a setup, e.g. when a background signal is present. In the latter case parameters of the discrete Fourier transform (DFT) have a huge impact on the SNR, as will be shown later.

To at least partly eradicate parameter influence on the SNR and allow some comparison between different NMR setups, the sensitivity S was introduced, as the measured SNR (SNR_{exp}) per sample concentration or amount [1–3]. The inverse of the sensitivity is the limit of detection (LOD), i.e. the sample amount necessary to obtain a SNR_{exp} of one, although many authors use a definition where the SNR_{exp} should be equal to three (e.g. [4–6])

$$\begin{aligned} LOD^c &= \frac{3c_s}{SNR_{exp}} \\ LOD^m &= \frac{3n_s}{SNR_{exp}} \end{aligned} \quad (1)$$

where c_s and n_s are the observed spin molar concentration (in M) and spin molar amount (in mol), respectively. As this definition completely ignores measurement parameters, the LOD can be easily decreased by adjustments to measurement parameters. The most obvious way to do that is to use signal averaging to enhance SNR by a factor of \sqrt{scans} , where $scans$ is the number of summed measurements [7], which increases the total measurement time. Therefore, more advanced versions of S and LOD definitions, called normalized S (nS) and normalized LOD ($nLOD$), try to mitigate the influence of signal averaging by a division of SNR_{exp} with the square root of the total measurement time [1], which relates the LOD to the measurement time t

$$nLOD_{old}^m = \frac{3n_s\sqrt{t}}{SNR_{exp}} \quad (2)$$

Scaling with measurement time bears its own problems, like the influence of repetition delay on the total measurement time. The repetition delay is determined by the spin-lattice relaxation time and varies between samples. As we will show, for the frequency domain $nLOD$ the use of any time-normalization is even more problematic. Various other definitions of a LOD were given in NMR literature [4–6] and consistency is certainly not present in neither definition nor use of both quantities or even naming (see also Appendix B).

* Corresponding author.

E-mail addresses: p.lepucki@ifw-dresden.de (P. Lepucki), a.p.dioguardi@ifw-dresden.de (A.P. Dioguardi), d.karnaushenko@ifw-dresden.de (D. Karnaushenko), o.schmidt@ifw-dresden.de (O.G. Schmidt), h.grafe@ifw-dresden.de (H.-J. Grafe).

In this paper we want to present equations for the $nLOD$ in both time and frequency space, which we will call $nLOD_t$ and $nLOD_f$, respectively. We will start by an analysis of the theoretical SNR from two complementary equations. The parameters entering the equations will be divided into parameters of the measurement setup and other parameters. We will then use the SNR analysis to derive the $nLOD_t$ and we will see that one of the existing equations is equal to ours. Then the $nLOD_f$ will be derived through an analysis of the DFT, which will result in a new equation. We argue that $nLOD_f$ is by far more useful for the comparison of sensitivities of different systems and will show this on the example of published data for NMR microdetectors. Finally, we will present a standard for measurements with new or improved NMR setups and give an example on how to report a standard measurement for optimal comparability of the measured sensitivity.

2. Signal-to-noise ratio

The SNR in time domain (SNR_t) of a setup, measured after a 90° pulse, is phenomenologically described by [8,9]

$$SNR_{t, \text{Abragam}} = K\eta M_S \sqrt{\frac{\mu_0 Q \omega_0 V_C}{4Fk_B T_C \Delta f}}. \quad (3)$$

Due to difficulties with a proper measurement of the parameters K and η , Hoult and Richards derived a formula from first principles for solenoids and saddle coils [10]

$$SNR_{t, \text{Hoult}} = \frac{K(B_1)_{xy} V_S N_S \gamma^2 h^2 I (I+1)}{7.12 k_B T_S} \left(\frac{p}{F k_B T_C l \zeta \Delta f} \right)^{1/2} \times \frac{\omega_0^{7/4}}{(\mu \mu_0 \rho(T_C))^{1/4}}. \quad (4)$$

where h is Planck's constant, k_B the Boltzmann constant and μ_0 the permeability of free space. The two equations are complementary, not exclusive, and are both useful to understand influences on SNR_t . We kept the original parameter namings. The following parameters contribute:

- K : a numerical factor dependent on detector geometry, which is usually close to one for solenoids.
- V_C, V_S : coil volume and measured sample volume.
- η : the magnetic filling factor. In the general case the filling factor is the fraction of the produced magnetic field energy of the detector, which is stored in the sample [11,9,12,6]. For the case of a long solenoid it is well described by $V_S/2V_C$. The factor $1/2$ stems from the fact that only half of the linear oscillating field, namely the circular component oscillating with $+\omega$, can be used for excitation. By principle of reciprocity [10], a circular field as produced by spins induces only half of the current a linear field would induce.
- M_S : the available sample magnetization, as defined by sample volume and nuclear spin concentration.
- Q : the quality factor of the resonance circuit, which is heavily dependent on the resistance of the resonance circuit [13,14].
- ω_0 : the resonance frequency in rad/s.
- F : the noise factor of the signal chain, dominated by the first element in a signal chain [15,16], normally the preamplifier.
- T_C, T_S : the sample and coil temperatures.
- Δf : the receiver bandwidth, as set by the experimenter.
- $K(B_1)_{xy}$: the effective field over the sample volume produced by a unit current through the detector, which is a solenoid or saddle coil.
- N_S : number of resonating spins
- γ, I : gyromagnetic ratio and spin of the used nucleus

- ζ : is a proximity factor and attributes for the proximity effect. It depends on the wire and detector geometry.
- p, l : perimeter and length of the conductor
- μ, ρ : permeability and resistivity of the conductor

We need to distinguish between different types of parameter. The first group are parameters defining the measurement setup. These are $K, \eta, Q, F, K(B_1)_{xy}, \zeta, p, l$ and ρ and are the parameters which would be optimized for a new system. We will treat them as defining the system sensitivity, therefore we will name them system parameters. We exclude the resonance frequency, since nowadays magnets up to 22 T are commercially available, some of which are sweepable, and ω_0 can be easily increased for a better SNR . ω_0 is better assigned to the second group.

The second parameter group are all parameters tunable for each experiment and includes $M_S, \omega_0, T_C, T_S, \Delta f, N_S, \gamma$ and I . We will call them measurement parameters. The influence of measurement parameters should be eliminated, if the intrinsic sensitivity of the setup is of interest. T_C, T_S, γ and I can be normalized through a measurement standard, which we will discuss at the end of the paper. The field strength dependence can be eliminated by a scaling of SNR to traditionally 600 MHz with $(600 \text{ MHz}/f_0)^{(7/4)}$ [1]. The influence of the remaining measurement parameters is normalized in the $nLOD$.

In frequency domain the SNR (SNR_f) is additionally dependent on the measured linewidth, defined as the full width at half maximum ($FWHM$) of a peak. Analytically one finds for the maximum signal in frequency domain S_{0f} [5]

$$S_{0f} = \frac{1}{2} S_{0,t} T_2^* \quad (5)$$

from the Fourier transform of an exponential decay, where T_2^* is the effective spin-spin relaxation time and $S_{0,t}$ is the maximum signal in time domain. Because of $FWHM = 1/(\pi T_2^*)$, the peak intensity S_{0f} will increase if the linewidth decreases. Noise is unaffected by T_2^* , therefore SNR_f will increase with smaller linewidths.

There is one last influence on SNR which should be heeded: the number of performed scans. It is common practice to increase the measured SNR by signal averaging, and the SNR grows with $\sqrt{\text{scans}}$ [7]. For a proper comparison between systems, the measured SNR should be divided by $\sqrt{\text{scans}}$. This correction was included e.g. in [5], but often - wrongly - instead of the number of scans the total measurement time t_{total} is used, as in [1]. t_{total} includes the acquisition time per scan Δt and the relaxation delay, which is why it is not a good scaling parameter.

3. Normalized limit of detection

The general definition of the LOD was given in Eq. 1. For the following normalization of LOD in time and frequency space, we will assume that the experiment performed was a free induction decay (FID) after a 90° pulse. For a smaller tip angle α we have to scale to a $\pi/2$ pulse with $1/\sin(\alpha)$. For experiments different than FID, which increase SNR , like a Carr-Purcell-Meiboom-Gill (CPMG) sequence, the SNR should be divided by the assumed gain in signal for one acquisition (done e.g. in [17]). We remind that c_s and n_s are the spin concentration and spin amount. Both quantities have to be calculated from sample concentration/amount times the number of resonating nuclei per molecule. For example, the spin amount of 1 mol of ethanol (C_2H_6O) is 6 mol for measurements on hydrogen but 2 mol for measurements on carbon for 100% ^{13}C enrichment. For not enriched samples, natural abundance of ^{13}C (1%) gives only 20 mmol of resonating spins.

nLOD in time domain

Normalizing the limit of detection for the time domain is straightforward. The only two experimental parameters still influencing the LOD_t are the set bandwidth of the receiver and the number of scans. A normalized LOD_t will be independent of both parameters, if the measured SNR_t is multiplied by $\sqrt{\Delta f}$ (see Eq. 3 and Eq. 4) and divided by \sqrt{scans} [7]. Here, SNR_t is defined as the intensity at $t = 0$ divided by $\sqrt{2}\sigma$, where σ is the standard deviation of noise. Then, the normalized LOD for the time domain is

$$\begin{aligned} nLOD_t &= \frac{LOD_t \sqrt{scans}}{\sqrt{\Delta f}} \\ nLOD_{t,600} &= nLOD_t \left(\frac{f_0}{600\text{MHz}} \right)^{7/4} \end{aligned} \quad (6)$$

where $nLOD_{t,600}$ is $nLOD_t$ scaled to 600 MHz, with f_0 in MHz. LOD_t is calculated from the measured $SNR_{t,exp}$ with Eq. 1. Eq. 6 was reported in a similar form in e.g. [6].

$nLOD$ in frequency space

For spectroscopy, frequency space is more significant and consequently the limit of detection should be also defined in frequency domain. The SNR can then be measured on the spectral peak of interest. This implies that now c_s and n_s are the spin concentration and spin amount for the selected spectral peak. Note that a splitting of the peak of interest due to J-coupling always reduces the measured SNR . A singlet is therefore always preferable, but since choosing a split line for SNR measurements does not inflate the measured SNR , but reduces it by a well defined amount, it is acceptable to measure SNR on a multiplett.

To normalize LOD_f we need to take a look at the discrete Fourier transform (DFT). The Fourier transform of a series of N discrete, complex, time-domain data points x_n is

$$X_k = \sum_{n=0}^{N-1} x_n (e^{-i2\pi nk/N}) \quad (7)$$

We can immediately see that a popular method to increase point density in frequency space, namely zero-filling, does not influence SNR_f at all, as it only adds zeros to the sum.

The DFT of random noise is again random noise, and the dependency of random noise in frequency space follows the dependency of random noise in time space with \sqrt{scans} and $\sqrt{\Delta f}$. In Fig. 1 we show that experimental frequency-domain noise has the same

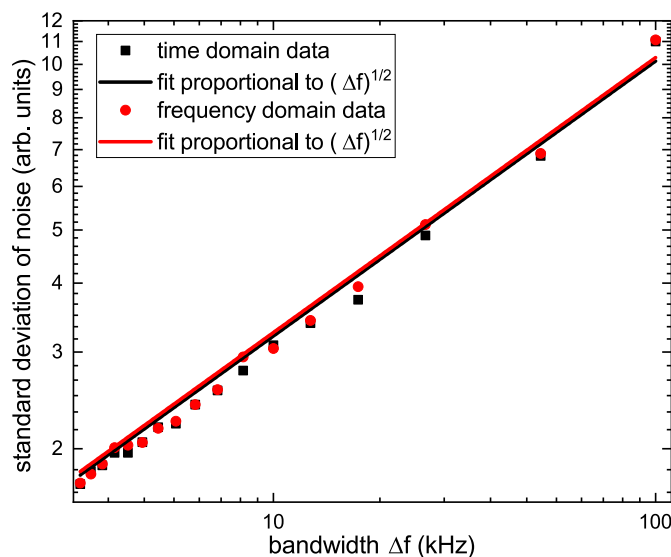


Fig. 1. Noise measurements with an empty NMR setup. Both noise levels show the same dependence. Parameters are: 300.125 MHz measurement frequency, 4096 points, 1 scan, 5 μ s pulse width.

bandwidth dependence as time-domain noise. The same result was obtained for simulated Gaussian noise.

For the signal, let us assume a single spectral line and the resonance frequency exactly matching the measurement frequency. In this scenario, the signal in time domain will be an exponential function with a fixed physical decay constant T_2^* . The mathematical decay constant, defined as the number of data points and not a time, will depend on the product of T_2^* and Δf . The peak signal after the DFT is a sum over all data points of the time domain. Therefore, the signal in frequency domain is proportional to $T_2^* \Delta f$, where T_2^* is influenced by the external field homogeneity, but Δf is chosen by the experimenter. Since the noise still scales as $\sqrt{\Delta f}$, the measured SNR_f is proportional to $\sqrt{\Delta f}$.

The number of data points N also has an influence on SNR_f . During the integration for the peak signal in frequency space, i.e. $f = 0$ Hz, the signal amplitude is constant after the noise level in the time domain is reached and every additional data point in time domain adds to noise, except zero-filling points, which add zero. We then have a similar situation as for signal averaging, with the difference that the signal stays constant while the noise level grows with \sqrt{N} after all signal is integrated. A good approximation for SNR_f is

$$SNR_f \propto SNR_t \frac{\Delta f T_2^*}{\sqrt{N}} \quad (8)$$

The time domain signal should occupy as many time domain data points as possible to maximize the peak signal in frequency domain. To achieve that we can minimize the number of noise points, i.e. make N small, or maximize the amount of signal points for constant N , i.e. decrease the dwell time per point, which is equal to an increase in bandwidth. The influence of both parameters on SNR_f is plotted in Fig. 2 for ^1H measurements on ethanol. Note also the linear dependence of SNR_f on the effective spin-spin relaxation rate and consequently the linewidth.

A similar dependence of SNR_f was published in [5,18], where they used the acquisition time per scan Δt . In our opinion, it is important to take N and Δf from the time domain for the correction. While Δt is defined by $N/\Delta f$, the use of the acquisition time distracts from the actual parameters and often is mistaken for the total measurement time, i.e. with signal averaging and T_1 relaxation. Additionally, zero filling adds to the number N , effectively increasing Δt , but does not influence the actual signal or noise levels, because during the DFT zero-filling points add zeros. Adding the effects of DFT to the $nLOD$ calculation and excluding the linewidth, the $nLOD_f$ reads

$$\begin{aligned} nLOD_f &= LOD_f \frac{\sqrt{\Delta f \sqrt{scans}}}{\sqrt{N}} \\ nLOD_{f,600} &= nLOD_f \left(\frac{f_0}{600\text{MHz}} \right)^{7/4} \end{aligned} \quad (9)$$

and LOD_f is calculated from measured $SNR_{f,exp}$ in accordance with Eq. 1.

4. Comparing NMR microdetectors

We want to present the usefulness of a $nLOD_f$ on the example of microdetectors for NMR spectroscopy, which include solenoids, planar coils, striplines and others. Such detectors have been under development since the early 90s due to their increased mass sensitivity compared to normal sized detectors. The interested reader can look into the matter in [6,46,47,1,48–50]. Usually the performance of such microdetectors is compared to normal detectors of the same research group, where the increase in SNR for a given sample mass is sufficient to show the better mass sensitivity of a microdetector (e.g. [51,21]). Only seldom a comparison to other

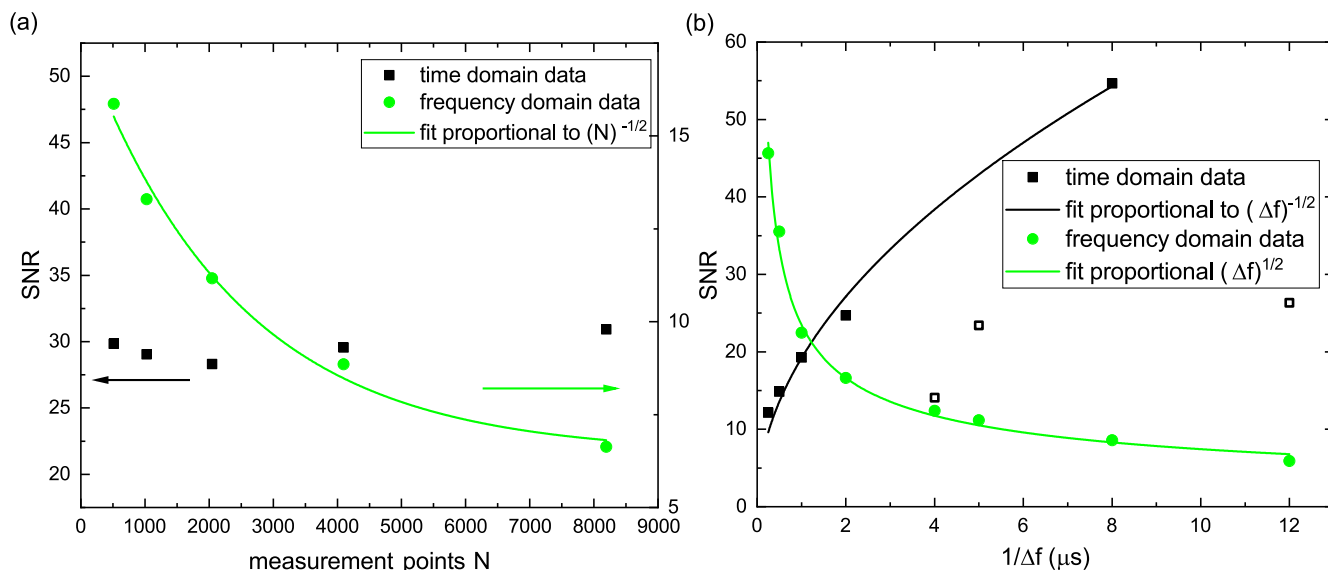


Fig. 2. ^1H measurements for SNR comparisons on pure ethanol. Starting parameters: 5 μs dwell time (200 kHz bandwidth), 299.97 MHz measurement frequency, 2048 measurement points N , 32 scans, 10 μs pulse width. In a) we varied N for the measurement and in b) the bandwidth. All SNR were calculated from experimental data. Some spectra had to be baseline corrected with a simple sine fit (excluding signal area). The noise level for the time SNR in a) was the average noise for all time domain measurements for this series, as the individual measurements showed large scattering due to random noise. The effect of random noise can also be seen in b) on the time domain data. Noisy time domain points in b) (open squares) were excluded from the fit.

published detectors is made. If such a comparison is made, the sensitivity is reported in many different ways, e.g. as SNR per acquisition time and molarity [52], LOD in $\text{nmol}/\sqrt{\Delta f}$ [6,19], nmol per acquisition time [4] and other variants. This inconsistency makes a judgment of detector performance nearly impossible. With the $n\text{LOD}_f$ defined in Eq. 9, an absolute value for the sensitivity of an NMR setup with a microdetector is given.

4.1. Scattering of presented data

Before we take a closer look at microcoil data, some remarks about the gathering and scattering of the presented data should be made. All of the presented $n\text{LOD}_f^m$ had to be calculated, because Eq. 9 is new. Exemplary calculations can be found in the Appendix. In the best case the measurement time Δt and the LOD as defined in [1] were given, in which case the $n\text{LOD}_f^m$ was obtained through a division of the reported LOD by measurement time. Which brings us to the point of calculating the $n\text{LOD}_f^m$ using the reported Δt instead of $N/\Delta f$. Only few authors provided a complete data set, consisting of SNR_{exp} , Δf , N , FWHM , sample type or amount of spins, and sample volume. In some cases SNR_{exp} or FWHM had to be estimated from published spectra. Measurement times were also seldom reported, which means the measurement time per scan had to be extracted from a plotted spectrum or FID, but both methods are prone to error, as FID or spectrum could be post-treated. If only SNR_t was given or extracted, $n\text{LOD}_f^m$ was calculated from the $n\text{LOD}_t^m$ by scaling with the linewidth. Also, we have to keep in mind that the flip angle has an influence on the planar magnetization and therefore signal strength. The standard for SNR calculations is a flip angle of 90° , but in chemical spectroscopy a flip angle of 30° is common to shorten the waiting time between consecutive scans. In the calculations always a flip angle of 90° was assumed, because the flip angle is seldom reported in publications not explicitly treating the SNR.

Additionally, note that the presented data points are slightly influenced by remaining setup components, not only by the intrinsic detector sensitivity. Spectrometers, preamplifiers, cables can all

be a source of additional noise, while the used type of resonance circuit (top-tuning or bottom-tuning) can make a factor of 3 difference in measured SNR. The presented data points reflect the sensitivity of a complete NMR setup, but the microdetector has the biggest influence on the sensitivity. We expect large scattering despite the fact that we only used publications which did provide enough data for an exact calculation or a good estimate.

Generally speaking, scattering between different detector types and NMR setups will always occur. For example, the average planar coil will always have a worse $n\text{LOD}$ than the average solenoid, but the planar coil can be used for applications where a solenoid is at a disadvantage. Furthermore, improved setups should have an improved sensitivity and therefore their $n\text{LOD}$ has to differ from older setups. In summary, a part of the scattering is due to the lack of a report standard and the use of a wrong normalization, but the majority is simply due to the different nature and intrinsic sensitivity of the detectors.

4.2. Old vs. new normalization

In Fig. 3 the $n\text{LOD}_f^m$ extracted from hydrogen spectra are plotted against the achieved FWHM of a detector. Data for plot a) was calculated using a LOD equation from [1] and scaled to 600 MHz with $(f_0/600 \text{ MHz})^{7/4}$. Data for plot b) was calculated using Eq. 9. In terms of detector quality this plot is very expressive, as it combines the sensitivity and resolution. This way the sensitivity of a setup can be judged in the context of the achievable resolution, which is especially useful for sensitivity estimation of wide-line measurements.

In both plots, the blue line marks the linear dependence of $n\text{LOD}_f^m$ on the linewidth (see Eq. 8) and its slope was chosen so that most published detectors lie above this line. The line should be treated as a guide to the eye. With further improvement of NMR systems, the slope will likely have to be adjusted. If a new microcoil, or in general a new setup, was made and no signal losses are present, the FWHM - $n\text{LOD}$ data point should lie near the blue line. Everything clearly above this line, where we set the limit to half an order of magnitude, can be improved further, e.g. by

Table 1

Old and new data points for the LOD in frequency space, together with linewidth. A plot of this data is given in Fig. 3a and b.

FWHM (ppb)	$LOD_{f,600}^m$ (nmol s ^{1/2})	$nLOD_{f,600}^m$ (nmol Hz ^{1/2})	source
<i>solenoids</i>			
200	0.20357	1.15	[19]
2.66	25.40444	16.93	[20]
33.88	0.01827	1.2	[21]
16	3.53239	1.1	[22]
1600	0.22892	25.19	[23]
40	0.98372	1.99	[24]
2	0.2646	0.26	[4]
2	0.30919	0.31	[25]
2.33	33.90132	8.27	[26]
1.04	0.09573	0.024	[17]
56.56	8.45877	57.08	[27]
3.6	0.69749	0.25	[28]
2175	4.24474	484.68	[29]
<i>striplines</i>			
1.16	9.52	9.52	[30]
1.6	0.73	0.76	[31]
5.77	1.45678	0.81	[32]
5.6	1.4	7.12	[33]
<i>helmholtz</i>			
3.58	22.5608	13.75	[34]
<i>planar</i>			
143	192.5855	446.69	[35]
14.33	37.92976	9.48	[18]
42	0.63942	1.81	[36]
23	27.81169	6.96	[37]
20000	4.12952	1088.2	[38]
56.66	116.93771	116.94	[39]
100	4.45655	27.17	[5]
388	1405.06319	936.6	[40]
7.5	22.2	0.49	[41]
7.17	5.00269	1.25	[42]
12.4	1380.01041	347.25	[43]
<i>saddle</i>			
3.04	27.47417	24.97	[44]
<i>rolled-up</i>			
22	1.24	3.81	[45], own
8	2.85739	0.44	[45], own

improving the quality factor of the detector. Data points near the line are of low-loss detectors, where the $nLOD_f^m$ is mainly limited by the linewidth. A data point clearly below this line indicates a microdetector that outperforms current microdetectors and the $nLOD_f^m$ calculation should be checked. If there is no error in the calculation, the setup shows unprecedented sensitivity.

We want to draw your attention to three features of plot a). Firstly, the green points were calculated from SNR_i without a correction with $FWHM$. Clearly this gives terrible scattering and the data points cannot be compared to ones calculated from SNR_f . Secondly, there is especially one point in plot a) far below the blue line, which is the planar coil with the highest $FWHM$. This point is from [38] and belongs to a planar coil fully integrated into a single chip transceiver. While at first glance it seems plausible that a single chip transceiver shows very low signal losses, three orders of magnitude of improvement seems a bit too much. Indeed, this point lies near the blue line when calculated with the new equation (Fig. 3b). Thirdly, from our work on rolled-up microcoils we got two data points measured with the same detector (red stars), but in different magnets with different spectrometers [45]. It seemed strange that the magnet with better linewidth and a cleaner setup showed a higher LOD . Therefore, we took a closer look at the LOD in frequency space and derived Eq. 9. In plot b), all three issues are not present anymore and most importantly, the $nLOD$ of the single rolled-up detector (red stars) shows a correct linewidth dependence. Overall scattering in plot b) is reduced, which we checked via the linear correlation coefficient r : it is -0.06 for Fig. 3a and 0.7 for Fig. 3b. After excluding all disputable points mentioned above (marked in green and from [38]), r is 0.65 for Fig. 3a and 0.91 for Fig. 3b. Therefore, Eq. 9 reduces scattering significantly.

5. Standard for sensitivity measurements and reports

Based on our discussion, we propose a report standard for the sensitivity of new or improved NMR setups. The report should contain one simple 90° pulse FID spectrum measured at room temperature and preferably on hydrogen, as it is the most sensitive nucleus. The spectrum should be a simple Fourier transform and should not be pretreated in any way. If zero-filling has been used,

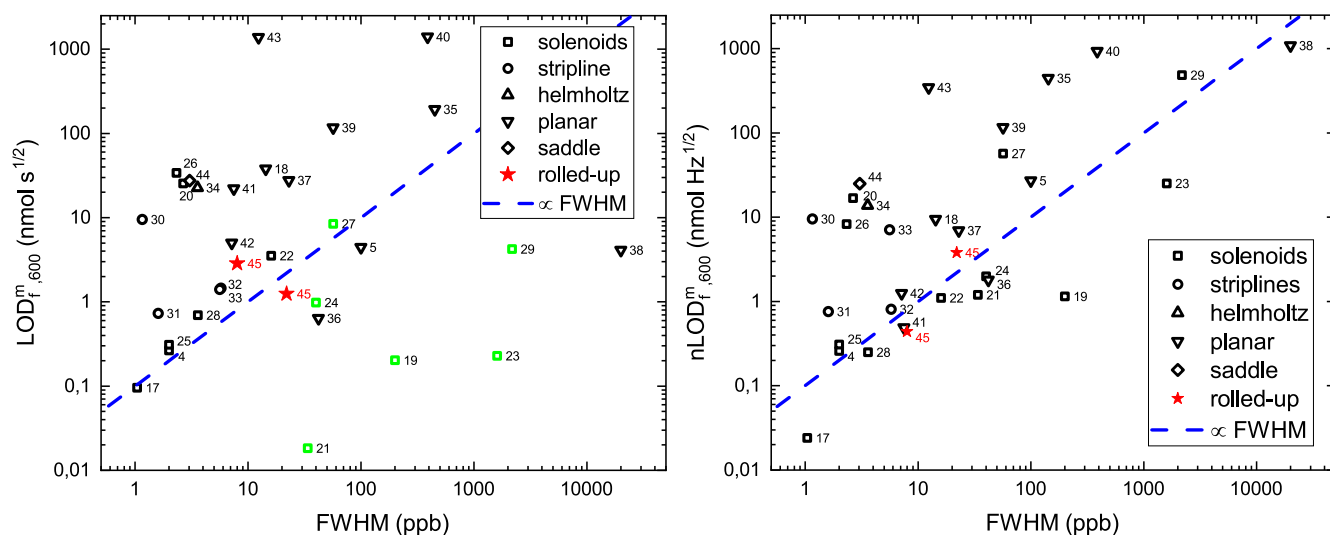


Fig. 3. $nLOD_f^m$ extracted from several publications (see Table 1) plotted against the linewidth. Each point represents a unique reported detector from different publications, except for the rolled-up microcoil, where it is the same detector in two different magnets. All used spectra were measured on 1H of liquid samples, except for the two largest linewidths, which were measured on solid samples. The blue lines show the linear dependence of $nLOD$ on $FWHM$. In (a), Eq. 2 from [1] was used for calculation, in (b) the new Eq. 9. The green points in (a) represent data calculated from SNR_i instead of SNR_f . Scattering of data is reduced with the new equation, see text.

these points should not be added to the amount of measurement points N . The SNR should be ideally measured on a singlet. The SNR on a multiplet is reduced, which results in an overestimation of the LOD (underestimation of sensitivity), therefore the use of a singlet standard is preferable. All important measurement parameters for a $nLOD_f^m$ calculation should be included in the figure caption. These parameters are:

- SNR of a peak of choice, optimally a singlet
- number of scans
- number of data points per scan
- the receiver bandwidth Δf (also called sweep width)
- the sample volume, sample type and molarity (where applicable)
- the linewidth of the peak of interest
- the measurement frequency f_0 .
- the used nucleus. The use of a nucleus different than hydrogen will require a further correction of the measured SNR to compare to literature data (see Eq. 4), which was not discussed in this paper.

These parameters are necessary to calculate a $nLOD_f^m$ which helps to judge even small changes to an NMR setup in terms of sensitivity and linewidth. It helps to understand improvements that were made or will have to be made when a new NMR setup is developed.

6. Summary

In this paper, we derived a formula for the comparison of NMR sensitivities between different NMR setups. The formula redefines the $nLOD$ in frequency space to be mathematically correct. For the mass LOD it now reads

$$nLOD_f^m = \frac{3n_s \sqrt{\Delta f}}{SNR_f \sqrt{N}} \quad (10)$$

where n_s is the measured sample amount in mol, Δf is the set receiver bandwidth, SNR_f is the measured signal to noise ratio for one scan in frequency space and N is the number of measurement points per scan. We stress that a spectrum used for the $nLOD_f$ calculation should be a simple DFT of the time domain data and recommend the use of hydrogen nuclei for measurements. We applied the new equation to data extracted from several publications treating microdetectors for NMR spectroscopy, and showed that it indeed describes detector performance independent of measurement parameters, but only based on detector properties and remaining system parameters. In order to make comparisons of the sensitivity between different publications easier, we also proposed a standard for measurements with new NMR setups and for the reporting on these. We believe that this standard will come in handy for future optimization of NMR setups and hope other authors will agree with us.

Declaration of Competing Interest

The authors declare that they have no known competing financial interests or personal relationships that could have appeared to influence the work reported in this paper.

Acknowledgement

This work was supported by the Leibniz-association (Leibniz-Transfer Program T62/2019).

Appendix A. Calculation of nLODs

The newly calculated nLODs have the unit $\text{nmol}\sqrt{\text{Hz}}$ (see Eq. 9). If the unit is $\text{nmol Hz}^{-1/2}$, the LOD was given by the authors and was calculated with a wrong equation.

Some publications gave SNR_t . In this case the $nLOD_t$ was calculated, scaled to 600 MHz and then transformed into $nLOD_f$ by multiplying with $\pi FWHM$. The reason is that the linewidth is in most cases determined by the coil susceptibility, therefore a higher field would give a higher absolute $FWHM$. This is not included in the $\omega^{7/4}$ factor.

A.1. Solenoid [21]

$FWHM$: 33.88 ppb from 1.5 Hz at 44.4 MHz, given

SNR : 10.3, but time domain, given

V_{sample} : 1.2 nl, given

n_s : from volume and sample type (water, 1 g/ml and 18.01 g/mol times two for protons), gives 133.26 nmol measurement time: time domain data, bandwidth 500 Hz.

$nLOD$: time domain data. here we need to additionally multiply by $\pi FWHM$ to get $nLOD$ in frequency space. Then the $nLOD$ is 1.79 $\text{nmol}\sqrt{\text{Hz}}$ at 44.4 MHz in time domain, 1.2 $\text{nmol}\sqrt{\text{Hz}}$ @ 600 MHz

A.2. Stripline [30]

$FWHM$: 1.16 ppb from 0.7 Hz @ 600 MHz, given

SNR : 189 on anomeric proton of sucrose, given

V_{sample} : 600 nl, given

n_s : 600 nmol, given

measurement time: 1 s (total time per scan: 5.5 s)

$nLOD$: 22.3 $\text{nmol Hz}^{-1/2}$, given. We think this not to be correct, the LOD was calculated using the total time per scan (5.5 s), not the acquisition time (1 s). $nLOD$ corrected by $1/\sqrt{5}$ is 9.52 $\text{nmol}\sqrt{\text{Hz}}$.

A.3. Helmholtz [34]

$FWHM$: 3.58 ppb, given

SNR : 1086, given

V_{sample} : 79 nl, given. Water sample

n_s : calculated to 8.7729 μmol

measurement time: 1.64 s, given

$nLOD$: calculated to 31.04 $\text{nmol Hz}^{-1/2}$ @ 500 MHz, which is a factor of 2 bigger than the reported value. Probably missed a 2 in calculation of sample amount. New: 18.92 $\text{nmol}\sqrt{\text{Hz}}$ @ 500 MHz, 13.75 $\text{nmol}\sqrt{\text{Hz}}$ @ 600 MHz

A.4. Planar 2008 [35]

$FWHM$: from given effective T_2 (11.1 ms) calculated to 28.68 Hz @ 200 MHz or 143 ppb

SNR : 20 for 256 scans, given. For one scan 1.25

V_{sample} : 2.07 μl , defined through active volume

n_S : from given spin density ($54.21 \times 10^{25} \text{ m}^{-3}$) and volume to 900 nmol

measurement time: 30 min for 256 averages? would be 7 s, but including T_1 effects. On page 451 they use 0.5 s for a calculation.

nLOD: $1317 \text{ nmol Hz}^{-1/2}$, given. Calculated $3054.7 \text{ nmol}\sqrt{\text{Hz}}$ @ 200 MHz, $446.69 \text{ nmol}\sqrt{\text{Hz}}$ @ 600 MHz

A.5. Saddle [44]

FWHM: 1.52 Hz @ 500 MHz → 3.04 ppb, given

SNR: 722.75, given

V_{sample} : 82 nl, given, water(?)

n_S : calculated to 9.106 μmol

measurement time: 1.1 s, given

nLOD: $18.78 \text{ nmol Hz}^{-1/2}$, given for old equation. New equation gives $34.36 \text{ nmol}\sqrt{\text{Hz}}$ @ 500 MHz, calculation based on water. I.e. the authors forgot to take the second water proton into account. $24.97 \text{ nmol}\sqrt{\text{Hz}}$ @ 600 MHz

A.6. Rolled-up [45]

FWHM: 22 ppb

SNR: 21.1, 1 scan

V_{sample} : 1.5 nl, ethanol

n_S : calculated to 51.4 nmol

measurement time: 0.325 s

nLOD: $1.24 \text{ nmol Hz}^{-1/2}$, $3.81 \text{ nmol}\sqrt{\text{Hz}}$

Appendix B. List of published data

Here we provide a list of data from the cited microcoil publications, see Fig. B.4. This list is by no means complete and refers only to the articles which provided enough data to calculate a nLOD. Note that the only consistently reported value for coil characterization is the SNR. LODs were only reported in half of the used articles,

and there not consistently. Especially the time is defined differently.

References

- [1] M.E. Lacey, R. Subramanian, D.L. Olson, A.G. Webb, J.V. Sweedler, High-Resolution NMR Spectroscopy of Sample Volumes from 1 nl to 10 μl , Chem. Rev. 99 (10) (1999) 3133–3152, <https://doi.org/10.1021/cr980140f>.
- [2] D.L. Olson, J.A. Norcross, M. O'Neil-Johnson, P.F. Molitor, D.J. Detlefsen, A.G. Wilson, T.L. Peck, Microflow NMR: Concepts and Capabilities, Anal. Chem. 76 (10) (2004) 2966–2974, <https://doi.org/10.1021/ac035426l>.
- [3] A.G. Webb, Radiofrequency microcoils for magnetic resonance imaging and spectroscopy, J. Magn. Reson. 229 (2013) 55–66, <https://doi.org/10.1016/j.jmr.2012.10.004>.
- [4] D.L. Olson, T.L. Peck, A.G. Webb, R.L. Magin, J.V. Sweedler, High-Resolution Microcoil 1H-NMR for Mass-Limited, Nanoliter-Volume Samples, Science 270 (5244) (1995) 1967–1970, <https://doi.org/10.1126/science.270.5244.1967>.
- [5] C. Massin, F. Vincent, A. Homsy, K. Ehrmann, G. Boero, P.-A. Besse, A. Daridon, E. Verpoorte, N.F. de Rooij, R.S. Popovic, Planar microcoil-based microfluidic NMR probes, J. Magn. Reson. 164 (2) (2003) 242–255, [https://doi.org/10.1016/S1090-7807\(03\)00151-4](https://doi.org/10.1016/S1090-7807(03)00151-4).
- [6] V. Badilita, R.C. Meier, N. Spengler, U. Wallrabe, M. Utz, J.G. Korvink, Microscale nuclear magnetic resonance: a tool for soft matter research, Soft Matter 8 (41) (2012) 10583, <https://doi.org/10.1039/c2sm26065d>.
- [7] C.P. Slichter, Principles of magnetic resonance, Springer Verlag, 1989.
- [8] A. Abragam, Principles of nuclear magnetism, Oxford Clarendon Press, 1961.
- [9] H.D.W. Hill, R.E. Richards, Limits of measurement in magnetic resonance, J. Phys. E: Sci. Instrum. 1 (10) (1968) 977–983, <https://doi.org/10.1088/0022-3735/1/10/202>.
- [10] D.I. Hoult, R.E. Richards, The signal-to-noise ratio of the nuclear magnetic resonance experiment, J. Magn. Reson. (1969) 24 (1) (1976) 71–85, [https://doi.org/10.1016/0022-2364\(76\)90233-x](https://doi.org/10.1016/0022-2364(76)90233-x).
- [11] N. Bloembergen, R.V. Pound, Radiation Damping in Magnetic Resonance Experiments, Phys. Rev. 95 (1) (1954) 8–12, <https://doi.org/10.1103/PhysRev.95.8>.
- [12] F.D. Doty, G. Entzminger, C.D. Hauck, J.P. Staab, Practical Aspects of Birdcage Coils, J. Magn. Reson. 138 (1) (1999) 144–154, <https://doi.org/10.1006/jmre.1998.1703>.
- [13] T.R. Kuphaldt, Lessons In Electric Circuits, Volume II - AC, public license, 2002.
- [14] C.K. Alexander, M.N.O. Sadiku, Fundamentals of Electric Circuits, McGraw-Hill, 2006.
- [15] H.T. Friis, Noise Figures of Radio Receivers, in: Proceedings of the IRE, vol. 32, IEEE, 1944, pp. 419–422.
- [16] P. Poshala, K.K. Rushil, R. Gupta, Signal Chain Noise Figure Analysis Tech. rep., Texas Instruments Inc, 2014.

reference	1 st author	doi	Filling factor	Q	Ball Shift	Nutation	SNR	LOD	LOD equation	used time	sample type
30	J. Bart	10.1016/j.jmr.2009.09.007	✓	✓	✓	✓	✓	✓	$LOD = N / SNR_{\text{ss}} \sqrt{\Delta f}$		sucrose in D2O
35	N. Baxan	10.1016/j.crci.2007.07.002	✗	✗	✗	✗	✓	✓	$nLOD_m = 3 \text{ mol} \sqrt{(t_{\text{scan}}) / SNR}$	t_{scan} is total measurement time	choline in H2O
31	Y. Chen	10.1039/C7CP03933F	✗	✓	✓	✓	✓	✓	$nLOD_m = 3 n \sqrt{(t_{\text{exp}}) / SNR}$	t_{exp} is total measurement time	sucrose in H2O
19	V. Demas	10.1016/j.jmr.2007.08.011	✗	✓	✗	✓	✓	✓	$nLOD_m = 3 n \sqrt{(t_{\text{acq}}) / SNR}$	t_{acq} is total measurement time	ethanol in D2O
18	K. Ehrmann	10.1016/j.jmr.2005.08.018	✗	✓	✗	✓	✓	✓	SNR of 3 in 1h		H2O
32	G. Finch	10.1016/j.jmr.2015.11.011	✗	✓	✗	✓	✓	✓	$nLOD_o = 3 n \sqrt{(\Delta t) / SNR}$	Δt is total measurement time	sodium acetate in H2O
36	R. M. Fraila	10.1038/ncomms4025	✗	✗	✗	✗	✓	✓	$S_m = SNR / m \sqrt{(t_{\text{acq}})}$	t_{ac} is time for one scan	H2O
37	A. G. Goloshe	10.1063/1.1848659	✓	✓	✗	✗	✗	✗	$N_{\text{min}} = V_S N_S VSD / s_0$	VSD, s_0 : noise and signal at Chip output	H2O
38	M. Grisi	10.1063/1.4916206	✗	✗	✗	✗	✓	✗			H4F6NP, solid
20	R. Kc	10.1002/cmr.b.20152	✗	✗	✗	✗	✓	✗			sucrose in D2O
5	C. Massin	10.1016/S1090-7807(03)00151-4	✗	✓	✗	✓	✓	✓	$LOD_m = 3 \text{ mol} \sqrt{(N_{\text{acq}}) / SNR}$		H2O
39	C. Massin	10.1016/S0924-4247(01)00847-0	✗	✓	✗	✗	✗	✗			ethylbenzene
21	A. F. McDowell	10.1016/j.jmr.2007.06.008	✗	✗	✗	✗	✓	✗			H2O
23	T. Meier	10.1016/j.jmr.2015.05.007	✗	✓	✗	✓	✓	✗			H2O
22	R. Ch. Meier	10.1088/0960-1317/24/4/045021	✗	✓	✗	✗	✓	✓	$LOD = 3 N_s \sqrt{(t_{\text{exp}}) / SNR}$	t_{exp} is time for one scan	H2O
24	M. Mompean	10.1038/s41467-017-02575-0	✗	✗	✗	✓	✓	✓			GMP in D2O
4	D. L. Olson	10.1021/ac970972y	✗	✓	✗	✗	✓	✓	mol per time	old	menthol in CDCl3
25	D. L. Olson	10.1126/science.270.5244.1967	✗	✗	✗	✗	✓	✓	LOD = 3 mol/SNR per time		sucrose in D2O
40	L. Renaud	10.1016/S0924-4247(01)00914-1	✗	✓	✗	✗	✓	✗			H2O
26	J. A. Rogers	10.1063/1.118857	✗	✗	✗	✗	✓	✓			acetone
41	H. Ryan	10.1021/ac300204z	✗	✓	✗	✗	✓	✓	$nLOD_m = 3 N_s \sqrt{(t_{\text{exp}}) / SNR}$	t_{exp} is total measurement time	glucose in D2O
17	D. A Seeber	10.1063/1.1359190	✗	✓	✗	✗	✓	✗			H2O
33	M. Sharma	10.1016/j.jmr.2019.04.007	✗	✓	✗	✗	✗	✓	$nLOD_o = 3 n \sqrt{(\Delta t) / SNR}$	Δt is 1/linewidth	sodium acetate in H2O
27	L. O. Sillerud	10.1016/j.jmr.2006.04.005	✓	✓	✗	✓	✓	✗			H2O
34	N. Spengler	10.1088/0960-1317/24/3/034004	✗	✓	✗	✓	✓	✓	$nLOD_m = 3 n \sqrt{(t_{\text{acq}}) / SNR}$		H2O
42	J. E. Stocker	10.1109/10.641340	✗	✗	✗	✗	✓	✗			H2O
28	R. Subramani	10.1006/jmre.1998.1450	✗	✗	✗	✗	✓	✓	mol per time	old	sucrose in D2O
43	J. D. Trumbull	10.1109/10.817611	✗	✗	✗	✗	✓	✗			H2O
44	N. Wang	10.1088/1361-6439/aa7a61	✗	✓	✗	✗	✓	✓	$nLOD_o = 3 n \sqrt{(\Delta t) / SNR}$	Δt is effective acquisition time Per scan	H2O
29	K. Yamauchi	10.1016/j.jmr.2003.12.003	✗	✓	✗	✓	✓	✓	amount of spins to get SNR = 1 in one scan		PDMS, but measured linewidth is due to field inhomogeneities

Fig. B.4. List of reported values from the cited articles.

- [17] D.A. Seeber, R.L. Cooper, L. Ciobanu, C.H. Pennington, Design and testing of high sensitivity microreceiver coil apparatus for nuclear magnetic resonance and imaging, *Rev. Sci. Instrum.* 72 (4) (2001) 2171–2179, <https://doi.org/10.1063/1.1359190>.
- [18] K. Ehrmann, M. Gersbach, P. Pascoal, F. Vincent, C. Massin, D. Stamou, P.-A. Besse, H. Vogel, R.S. Popovic, Sample patterning on NMR surface microcoils, *J. Magn. Reson.* 178 (1) (2006) 96–105, <https://doi.org/10.1016/j.jmr.2005.08.018>.
- [19] V. Demas, J.L. Herberg, V. Malba, A. Bernhardt, L. Evans, C. Harvey, S.C. Chinn, R. S. Maxwell, J. Reimer, Portable, low-cost NMR with laser-lathe lithography produced microcoils, *J. Magn. Reson.* 189 (1) (2007) 121–129, <https://doi.org/10.1016/j.jmr.2007.08.011>.
- [20] R. Kc, I.D. Henry, G.H.J. Park, A. Aghdasi, D. Raftery, New solenoidal microcoil NMR probe using zero-susceptibility wire, *Concepts Magn. Reson. Part B: Magn. Reson. Eng.* 37B (1) (2010) 13–19, <https://doi.org/10.1002/cmr.b.20152>.
- [21] A.F. McDowell, N.L. Adolphi, Operating nanoliter scale NMR microcoils in a 1tesla field, *J. Magn. Reson.* 188 (1) (2007) 74–82, <https://doi.org/10.1016/j.jmr.2007.06.008>.
- [22] R.C. Meier, J. Höflin, V. Badilita, U. Wallrabe, J.G. Korvink, Microfluidic integration of wirebonded microcoils for on-chip applications in nuclear magnetic resonance, *J. Micromech. Microeng.* 24 (4) (2014) 045021, <https://doi.org/10.1088/0960-1317/24/4/045021>.
- [23] T. Meier, S. Reichardt, J. Haase, High-sensitivity NMR beyond 200,000 atmospheres of pressure, *J. Magn. Reson.* 257 (2015) 39–44, <https://doi.org/10.1016/j.jmr.2015.05.007>.
- [24] M. Mompeán, R.M. Sánchez-Donoso, A. de la Hoz, V. Saggiomo, A.H. Velders, M. V. Gomez, Pushing nuclear magnetic resonance sensitivity limits with microfluidics and photo-chemically induced dynamic nuclear polarization, *Nat. Commun.* 9(1). doi: 10.1038/s41467-017-02575-0.
- [25] D.L. Olson, M.E. Lacey, J.V. Sweedler, High-Resolution Microcoil NMR for Analysis of Mass-Limited, Nanoliter Samples, *Analyt. Chem.* 70 (3) (1998) 645–650, <https://doi.org/10.1021/ac970972y>.
- [26] J.A. Rogers, R.J. Jackman, G.M. Whitesides, D.L. Olson, J.V. Sweedler, Using microcontact printing to fabricate microcoils on capillaries for high resolution proton nuclear magnetic resonance on nanoliter volumes, *Appl. Phys. Lett.* 70 (18) (1997) 2464–2466, <https://doi.org/10.1063/1.118857>.
- [27] L.O. Sillerud, A.F. McDowell, N.L. Adolphi, R.E. Serda, D.P. Adams, M.J. Vasile, T. M. Alam, 1H NMR detection of superparamagnetic nanoparticles at 1T using a microcoil and novel tuning circuit, *J. Magn. Reson.* 181 (2) (2006) 181–190, <https://doi.org/10.1016/j.jmr.2006.04.005>.
- [28] R. Subramanian, M.M. Lam, A.G. Webb, RF microcoil design for practical NMR of mass-limited samples, *J. Magn. Reson.* 133 (1) (1998) 227–231, <https://doi.org/10.1006/jmre.1998.1450>.
- [29] K. Yamauchi, J.W.G. Janssen, A.P.M. Kentgens, Implementing solenoid microcoils for wide-line solid-state NMR, *J. Magn. Reson.* 167 (1) (2004) 87–96, <https://doi.org/10.1016/j.jmr.2003.12.003>.
- [30] J. Bart, J.W.G. Janssen, P.J.M. van Bentum, A.P.M. Kentgens, J.G.E. Gardeniers, Optimization of stripline-based microfluidic chips for high-resolution NMR, *J. Magn. Reson.* 201 (2) (2009) 175–185, <https://doi.org/10.1016/j.jmr.2009.09.007>.
- [31] Y. Chen, H.S. Mehta, M.C. Butler, E.D. Walter, P.N. Reardon, R.S. Renslow, K.T. Mueller, N.M. Washton, High-resolution microstrip NMR detectors for subnanoliter samples, *Phys. Chem. Chem. Phys.* 19 (41) (2017) 28163–28174, <https://doi.org/10.1039/c7cp03933f>.
- [32] G. Finch, A. Yilmaz, M. Utz, An optimised detector for in-situ high-resolution NMR in microfluidic devices, *J. Magn. Reson.* 262 (2016) 73–80, <https://doi.org/10.1016/j.jmr.2015.11.011>.
- [33] M. Sharma, M. Utz, Modular transmission line probes for microfluidic nuclear magnetic resonance spectroscopy and imaging, *J. Magn. Reson.* 303 (2019) 75–81, <https://doi.org/10.1016/j.jmr.2019.04.007>.
- [34] N. Spengler, A. Moazen-zadeh, R.C. Meier, V. Badilita, J.G. Korvink, U. Wallrabe, Micro-fabricated helmholtz coil featuring disposable microfluidic sample inserts for applications in nuclear magnetic resonance, *J. Micromech. Microeng.* 24 (3) (2014) 034004, <https://doi.org/10.1088/0960-1317/24/3/034004>.
- [35] N. Baxan, H. Rabeson, G. Pasquet, J.-F. Châteaux, A. Briguët, P. Morin, D. Graveron-Demilly, L. Fakri-Bouchet, Limit of detection of cerebral metabolites by localized NMR spectroscopy using microcoils, *C. R. Chim.* 11 (4–5) (2008) 448–456, <https://doi.org/10.1016/j.crci.2007.07.002>.
- [36] R.M. Fratila, M.V. Gomez, S. Sýkora, A.H. Velders, Multinuclear nanoliter one-dimensional and two-dimensional NMR spectroscopy with a single non-resonant microcoil, *Nat. Commun.* 5(1). doi: 10.1038/ncomms4025.
- [37] A.G. Goloshevsky, J.H. Walton, M.V. Shutov, J.S. de Ropp, S.D. Collins, M.J. McCarthy, Development of low field nuclear magnetic resonance microcoils, *Rev. Sci. Instrum.* 76 (2) (2005) 024101, <https://doi.org/10.1063/1.1848659>.
- [38] M. Grisi, G. Gualco, G. Boero, A broadband single-chip transceiver for multi-nuclear NMR probes, *Rev. Sci. Instrum.* 86 (4) (2015) 044703, <https://doi.org/10.1063/1.4916206>.
- [39] C. Massin, G. Boero, F. Vincent, J. Abenheim, P.-A. Besse, R.S. Popovic, High-q factor RF planar microcoils for micro-scale NMR spectroscopy, *Sens. Actuators A: Phys.* 97–98 (2002) 280–288, [https://doi.org/10.1016/S0924-4247\(01\)00847-0](https://doi.org/10.1016/S0924-4247(01)00847-0).
- [40] L. Renaud, M. Armenean, L. Berry, P. Kleimann, P. Morin, M. Pitaval, J. O'Brien, M. Brunet, H. Saint-Jalmes, Implantable planar rf microcoils for NMR microspectroscopy, *Sens. Actuators A: Phys.* 99 (3) (2002) 244–248, [https://doi.org/10.1016/S0924-4247\(01\)00914-1](https://doi.org/10.1016/S0924-4247(01)00914-1).
- [41] H. Ryan, S.-H. Song, A. Zaß, J. Korvink, M. Utz, Contactless NMR spectroscopy on a chip, *Anal. Chem.* 84 (8) (2012) 3696–3702, <https://doi.org/10.1021/ac300204z>.
- [42] J.E. Stocker, T.L. Peck, A.G. Webb, M. Feng, R.L. Magin, Nanoliter volume, high-resolution NMR microspectroscopy using a 60 μm planar microcoil, *IEEE Trans. Biomed. Eng.* 44 (11) (1997) 1122–1127, <https://doi.org/10.1109/10.641340>.
- [43] J.D. Trumbull, I.K. Glasgow, D.J. Beebe, R.L. Magin, Integrating microfabricated fluidic systems and NMR spectroscopy, *IEEE Trans. Biomed. Eng.* 47 (1) (2000) 3–7, <https://doi.org/10.1109/10.817611>.
- [44] N. Wang, M.V. Meissner, N. MacKinnon, V. Luchnikov, D. Mager, J.G. Korvink, Fast prototyping of microtubes with embedded sensing elements made possible with an inkjet printing and rolling process, *J. Micromech. Microeng.* 28 (2) (2017) 025003, <https://doi.org/10.1088/1361-6439/aa7a61>.
- [45] P. Lepucki, A.I. Egunov, M. Rosenkranz, R. Huber, A. Mirhajivarzaneh, D.D. Karnaushenko, A.P. Dioguardi, D. Karnaushenko, B. Büchner, O.G. Schmidt, H.-J. Grafe, Self-Assembled Rolled-Up Microcoils for nL Microfluidics NMR Spectroscopy, *Adv. Mater. Technol.* 6 (1) (2020) 2000679, <https://doi.org/10.1002/admt.202000679>.
- [46] C.J. Jones, C.K. Larive, Could smaller really be better? current and future trends in high-resolution microcoil NMR spectroscopy, *Anal. Bioanal. Chem.* 402 (1) (2011) 61–68, <https://doi.org/10.1007/s00216-011-5330-7>.
- [47] F.C. Schroeder, M. Gronquist, Extending the Scope of NMR Spectroscopy with Microcoil Probes, *Angew. Chem. Int. Ed.* 45 (43) (2006) 7122–7131, <https://doi.org/10.1002/anie.200601789>.
- [48] A.P.M. Kentgens, J. Bart, P.J.M. van Bentum, A. Brinkmann, E.R.H. van Eck, J.G.E. Gardeniers, J.W.G. Janssen, P. Knijn, S. Vasa, M.H.W. Verkuijlen, High-resolution liquid- and solid-state nuclear magnetic resonance of nanoliter sample volumes using microcoil detectors, *J. Chem. Phys.* 128 (5) (2008) 052202, <https://doi.org/10.1063/1.2833560>.
- [49] A.G. Webb, Microcoil nuclear magnetic resonance spectroscopy, *J. Pharm. Biomed. Anal.* 38 (5) (2005) 892–903, <https://doi.org/10.1016/j.jpba.2005.01.048>.
- [50] P. Lepucki, Development of self-assembled, rolled-up microcoils for nuclear magnetic resonance spectroscopy, Ph.D. thesis, TU Dresden, 2021.
- [51] G. Carret, T. Berthelot, P. Berthault, Inductive Coupling and Flow for Increased NMR Sensitivity, *Anal. Chem.* 90 (19) (2018) 11169–11173, <https://doi.org/10.1021/acs.analchem.8b01775>.
- [52] J.R. Krug, R. van Schadewijk, F.J. Vergeldt, A.G. Webb, H.J.M. de Groot, A. Alia, H. V. As, A.H. Velders, Assessing spatial resolution, acquisition time and signal-to-noise ratio for commercial microimaging systems at 14.1, 17.6 and 22.3 T, *J. Magn. Reson.* 316 (2020) 106770, <https://doi.org/10.1016/j.jmr.2020.106770>.